A first approach of the influence of the forecasting horizon in the electricity generation simulation of a solar tower plant

Joaquín Alonso-Montesinos[1, 2], Jesús Polo[3], Jesús Ballestrín[4], Javier Barbero[1], Gabriel López[5], Aitor Marzo[6, 7] and Francisco Javier Batlles[1, 2]

[1] Department of Chemistry and Physics, University of Almería, 04120 Almería, Spain

[2] CIESOL, Joint Centre University of Almería-CIEMAT, 04120 Almería, Spain

[3] Photovoltaic Solar Energy Unit (Renewable Energy Division, CIEMAT), 28040 Madrid, Spain

[4] Concentrating Solar System Unit (Plataforma Solar de Almería, CIEMAT), 04200 Almería, Spain

[5] Department of Electrical and Thermal Engineering, Design and Projects, University of Huelva, 21004, Huelva, Spain

[6] CDEA, University of Antofagasta, 02800 Antofagasta, Chile

[7] Solar Energy Research Center (SERC-Chile), Santiago (Chile)

Abstract

Solar power plants are very interested in the prediction of power net generation and the instabilities that can affect the production of the plant. System Advisor Model (SAM) is widely used to simulate the behavior of concentration solar power plants, where different inputs parameters can be considered for simulations. Reliable short-term forecasting of the solar resource has significant positive consequences since it helps the planning of power plant operators for power dispatch and assess the plant reliability and the market trends. In this work, we quantify the accuracy of the electricity predictions of a solar power plant at different hour-scale, by using the solar irradiance forecasting obtained from Meteosat satellite images. For that, we have simulated the power generation of a solar power plant taking as input the solar irradiance forecasting with the purpose to determine the best forecast horizon time. The main novelty in this work is the analysis on the impact of short-term forecasting of DNI in the plant energy output at different forecasting horizons in solar tower plants with large thermal storage systems.

Keywords: Solar power plant, power net generation, SAM, satellite images, forecasting,

Introduction

The growing human population is causing an ever-increasing demand for conventional energy resources, which results in environmental negative effects. Renewable energies offer a viable and potent solution to counter the effects of this problem since they are pollution free, inexhaustible and affordable. In this context, solar energy technologies are growing in the last two decades being an alternative of conventional ways to produce electricity. Before constructing a solar power plant, several simulations are carried out to determine the best emplacements where technology can optimize the final production. System Advisor Model (SAM) is a software, which allows to determine a complete list of features to consider a plant in a concrete region. Developed and delivered at no cost by NREL (National Renewable Energy Lab), it has become the standard model for calculating the performance of solar thermal and photovoltaic plants since it has proven high reliability and performance compared to TRNSYS libraries designed for modeling CSP plants (Dobos et al., 2014; Wagner, 2008; Wagner and Gilman, 2011). Once that the solar plant has been built, the operation mode plays an important role. Decisions can increase the optimization of the plant and, subsequently, the electricity production and grid-power integration. Solar irradiance predictions are one of the best techniques to introduce in the operator systems for determining the future episodes that can affect the plant working. Concretely, Meteosat Second Generation (MSG) images are commonly used in the meteorological field, providing images every 15 mins, serving as relevant data for many researchers, for predicting the atmospheric conditions in short and large temporal scales (Alonso-Montesinos and Batlles, 2015; Boulifa et al, 2015).

In this work, we present a first approximation of the electricity generation simulation, where satellite predictions are used as input of the SAM simulation software. The aim is to obtain some deterministic characteristics for the choosing of the best forecasting horizon time, which would be very useful in the management and optimization of a solar power plant.

Selection and/or peer review under responsibility of Scientific Committee
doi:10.18086/eurosun2018.09.05 Available at http://proceedings.ises.org

Data acquisition and solar plant design

Radiation data are obtained from a radiometric station placed at the CIESOL building at the University of Almería, Spain (36.8º N, 2.4º W, at sea level). The meteorological station has a two-axes solar tracker (2AP Kipp&Zonen) above which direct, diffuse and global radiation sensors are installed. Furthermore, we collect images from a Meteosat Second Generation (MSG) satellite station, also placed on the roof of the CIESOL building. Radiation data are collected every minute. For the forecasting radiation, MSG satellite channels are collected every 15 minutes for 2013 and 2014 years.

The solar tower plant performance has been modeled with the System Advisor Model (SAM). SAM is a free and open source tool developed and distributed by the National Renewable Energy Laboratory (NREL) for estimating the energy production of different renewable energy systems (Dobos et al., 2014). In this work, the specific module for molten salt power tower systems is used (Neises and Wagner, 2012; Wagner, 2008). For the simulation of the solar power plant, one molten salt solar tower plant is selected as reference: Gemasolar, which is as a small plant with a very large thermal storage system. According to the case studies reported by NREL, the uncertainty in the annual production of Gemasolar plant computed with SAM is around 2.4%. Gemasolar has a total solar field area of 305401 m^2, the tower height is 140 meters with a total of 2650 heliostats. The technology is based on central receiver, using $NaNO_3$-KNO_3 as heat transfer fluid. The power block has 19.9 MWe and the total capacity for storage is 15 hours.

Methodology

This section introduces the methodology for power gross output of a central tower plant, combining remote sensing techniques SAM simulations.

3.1. Intra-hour DNI forecasting

For power gross output, it is necessary to carry out a solar radiation forecasting to know the radiation level available in the near future. For that, three consecutive images are processed to determine the vectors that identifies the pixel motion along the time based on cloud detection. Figure 1 shows a MSG satellite image, where the raw image (upper image) represents the Iberian Peninsula, focusing the interest in the CIESOL area (marked in red and presented in the bottom-left image), and the final image represents the identification of clouds in this area.

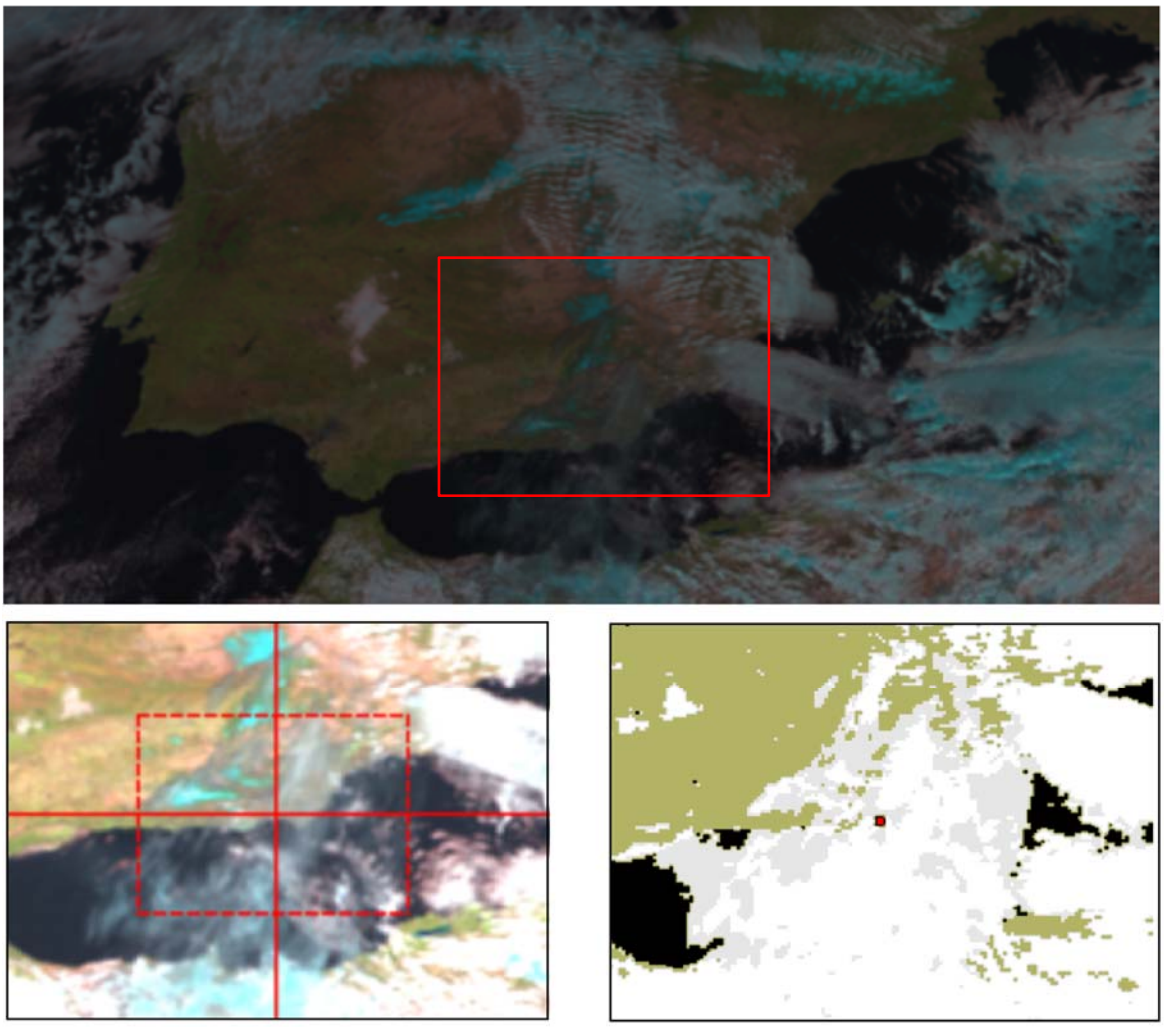

Fig. 1: MSG satellite image obtained on 10th February 2018 at 12:00 hours.

For each image collected every 15 minutes, 5 channels are used from the total 11 spectral channels. These channels are VIS 0.6, VIS 0.8, IR 3.9, IR 10.8 and IR 12.0. The images received are reduced, taking a 121x161 pixel raster image is taken, centred on the University of Almería. After that, an algorithm for detecting the presence of any clouds is applied in the various atmospheric layers of the raster map, considering full raster image (Escrig et al. 2013). With the cloud detection carried out in the three consecutive images, it is determined the cloud motion vectors. When vectors are calculated, the estimation of solar irradiance is obtained from the last image applying the Heliosat-2 method (Rigollier et al. 2000). Basically, this method considers the DNI estimation under cloudless skies for next applying an attenuation factor determined by presence of clouds. The expression which represents this approach can be defined as follows:

$$DNI = DNI_{clear\ sky} K_{cs} \qquad \text{(eq. 1)},$$

where $DNI_{clear\ sky}$ is the DNI predicted for a clear sky condition using the ESRA model and K_{cs} is the attenuation factor considering the presence of clouds.

In order to determine the value of $DNI_{clear\ sky}$, eq. 2 defines the expression to obtain the aforementioned value.

$$DNI_{clear\ sky} = I_0\ \varepsilon\ \sin(\alpha) T_{rb}(\alpha) \qquad \text{(eq. 2)},$$

where I_0 is the solar extraterrestrial radiation, ε is the correction used for the variation in the sun-earth distance from its mean value, α is the solar altitude angle and $T_{rb}(\alpha)$ is an expression which related the Linke Turbidity factor and the Rayleigh optical thickness, as a function of the α angle.

When $DNI_{clear\ sky}$ is obtained for cloudless skies, the last step for estimating the DNI value is to obtain the K_{cs} value through Heliosat 2 method which employs satellite images to calculate atmospheric attenuation (Rigollier et al. 2004; Alonso-Montesinos et al. 2015). The next expression shows the process to determine this attenuation factor at the pixel level:

$$\begin{aligned} &n < -0.2, K_{cs} = 1.2 \\ &-0.2 < n < 0.8, K_{cs} = 1 - n \\ &0.8 < n < 1.1, K_{cs} = 2.0677 - 3.667\, n + 1.667\, n^2 \\ &n > 1.1, K_{cs} = 0.05 \end{aligned} \qquad \text{(eq. 3)},$$

where n is the cloud index, obtained using the albedo retrieved from satellite image.

After that, there are two matrices, each with 121x161 pixels: one matrix corresponds to the $DNI_{clear\ sky}$ estimations whereas the other one represents/corresponds to the K_{cs} factor, both of them at pixel level. Therefore, the next step consists of determining the future DNI values. As one motion represents a 15-minute prediction, 12 motions are practiced to obtain a forecast from 15 to 180 minutes. Consequently, we have applied cloud motion vectors to each pixel of the raster image.
Therefore, for having a final DNI forecasting, when the K_{cs} pixels are moved, the $DNI_{clear\ sky}$ is estimated for the future moments and for a cloudless sky in all the pixels of the satellite raster image (Alonso-Montesinos et al. 2015), ending with the product between the $DNI_{clear\ sky}$, estimated in a pixel, and the K_{cs}, in the same pixel, generating the final DNI forecast.

3.2. Power plant simulation

After obtaining the DNI forecasting from 15 minutes to three hours, we simulate the power net production of a central tower solar power plant including the predictions obtained from satellite images. The aim is to compare the output gross production using each DNI prediction and the real DNI value to compare the differences, due to we simulate that Gemasolar plant is located in the CIESOL emplacement. Due that, we can use measured data from CIESOL's radiometric station.

The simulations are undertaken by means of the SAM software. The results obtained are then used to determine the best forecasting horizon by analyzing the impact of meteorological input compared to the experimental irradiance. For this work, the extinction model was used by default according to 25 km of visibility, not considering atmospheric attenuation measurements. This impact can be included in the operation and decisional way of a solar power plant management control system. The first results show that the predicted and real scenarios follow an interesting trend that can be deterministic in the choosing of the best forecasting time-scale applied in a solar power plant.

Results

Before to present the graphs for the two different plants, the trend between DNI experimental values and DNI forecasting values is analyzed. This result is the first parameter considered for determining the accuracy of the prediction model. Fig. 2 represents the total DNI for one year using experimental data against the DNI for the same year using the 12 predictions each one for 15 minutes, in an interval that goes from 15 to 180 minutes.

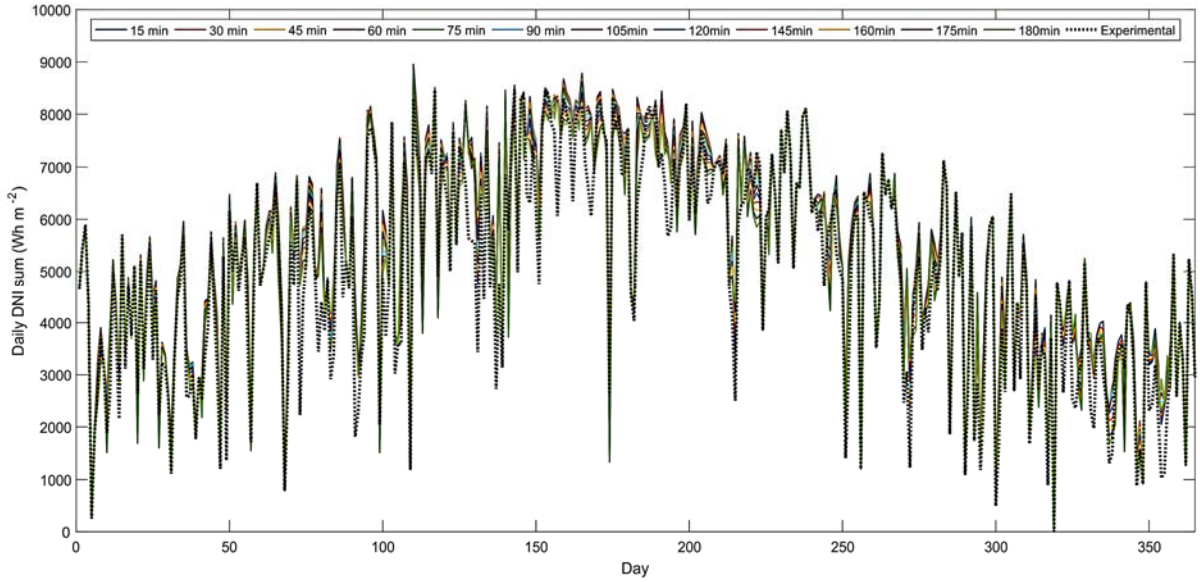

Fig. 2: Daily DNI for UAL emplacement.

In general, the main and important characteristic is the similitude between experimental and predicted data. This fact indicates the good concordance obtained from predictions using MSG images regarding to the measured DNI values. The trend goes from lower values (first and last part of the graph) that corresponds with winter days, reaching an average daily DNI value of 3000 Wm^{-2}, whereas for central days in the year (corresponding to summer days) this value is centered in 7000 Wm^{-2}. Obviously, there are important oscillations occasioned by clouds covering the surface of study, but they are well represented by the satellite predictions.

Considering the forecast method suitable according the results observed, the next consideration is to analyze the impact of the forecast interval in CSP plants. To represent the degree of concordance between the energy output obtained from simulation using real DNI values and obtained from simulation using DNI predictions, it has been developed one graph for the CSP plant.

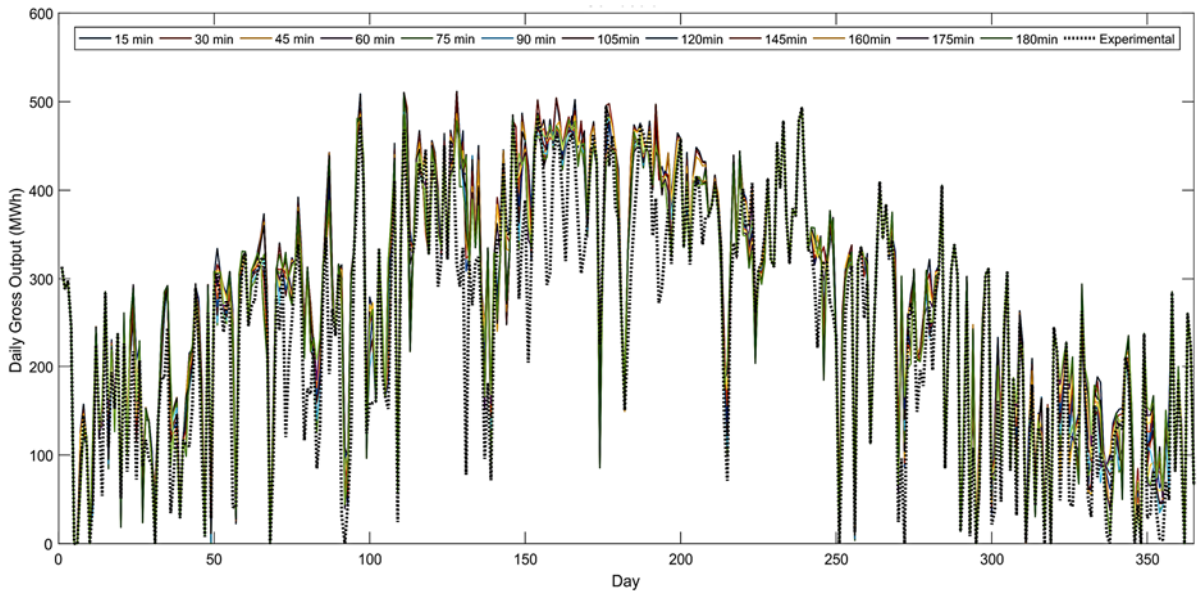

Fig. 3: Forecasted and simulated daily gross output for the UAL emplacement.

The daily gross energy output for Gemasolar plant follows a similar pattern than daily DNI, however, the oscillations present a lower amplitude, thanks to the plant's capability for producing energy using the heat stored in the molten salt tanks. The peak energy output values appear in summer where there are more hours of sunshine, reaching values near to 500 MWh. Moreover, the results show that the forecasting energy is in general agreement with the experimental in terms of the dynamics along the year. However, the forecasted energy has a trend to overestimate the energy. More detailed, green line is the more visible along the year, so, the other predictions present better approximations.

The accuracy of the predictions is analyzed in terms of both the root mean square error (RMSE) and mean bias error (MBE) between the predicted values Y_{est} and the measured ones, Y_{mea}. They are expressed as a percentage of the mean value of the latter, $\bar{Y}_{mea}$. The RMSE gives information about how concentrated the data are around the line of best fit and the MBE shows the tendency of the model to provide over- or under- estimation predictions. They are calculated according to Eqs. 4 and 5:

$$RMSE(\%) = \frac{100}{\bar{Y}_{mea}}\sqrt{\frac{1}{N}\sum_{i=1}^{N}(Y_{est} - Y_{mea})^2} \quad \text{(eq. 4)},$$

$$MBE = 100\frac{\frac{1}{N}\sum_{i=1}^{N}(Y_{est} - Y_{mea})}{\bar{Y}_{mea}} \quad \text{(eq. 5)}.$$

Figure 4 shows the relative metrics for the performance in daily basis, the MBE and the RMSE for Gemasolar plant.

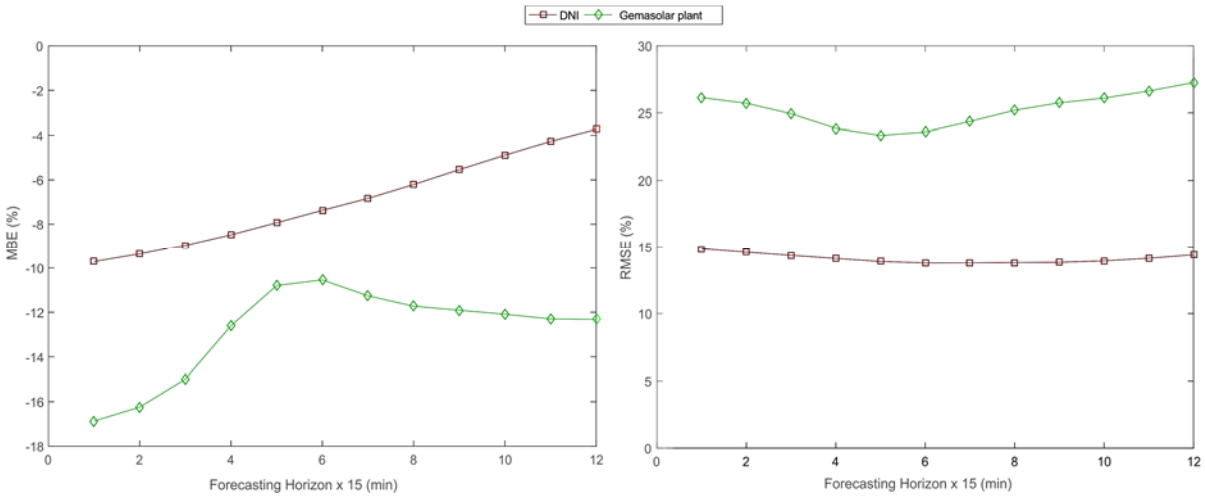

Fig. 4: MBE and RMSE results for the predictions from 15 minutes to 2 hours in Gemasolar plant.

The bias of the forecasted DNI presents a monotonically increase trend with the forecasting horizon while the RMSE exhibits an almost constant value of around 15% for daily values and for any forecasting horizon The bias clearly shows the overestimation tendency of all the forecasting horizons corresponding to the daily power output predictions. However a minimum bias and RMSE can be observed at around 75 and 90 minutes of forecasting horizon. Similarly, the RMSE decreases with the forecasting horizon till 90 minutes where it is placed around 24% in daily basis for both plants. Beyond 90 minutes, the RMSE (%) turns to an increase trend with the forecasting horizon. These results would suggest an optimum forecasting horizon for this type of solar tower plants with large thermal storage systems.

Moreover, it is important to focus the attention in one particular because of the influence of the prediction can play a deterministic role for adapting the CSP plant management.

Conclusions

In this work, a novel CSP power output forecasting has been presented, where satellite images along with the SAM simulation software are used to predict DNI values from 15 minutes to three hours.

A prototype of central tower power plant based on the Gemasolar plant and located at the University of Almería (Spain), where measured and predicted DNI are available, is used to undertake the simulations

The results obtained analyzing the full year of DNI prediction show a good concordance between measured and predicted values. In general terms, the DNI is overestimated along with RMSE values lower than 15% for all forecast horizons.

The power output is overestimated about a 10-17%. Furthermore, the results manifest a best approximation at 90-min horizon, with a MBE value of 12% and a RMSE value of 23%. In this respect, the molten salt thermal storage can modify the behavior of the DNI forecasting error, presenting better results within this specific horizon interval.

Therefore, this work has left in evidence that forecasting horizon plays an important role in the power output forecasting that can be decisive in the study of viability and management of a CPS plant.

Acknowledgements

This project has been financed by Projects (ENE2017-83790-C3-1, 2 and 3, and ENE2014-59454-C3-1, 2 and 3), which were funded by the Ministerio de Economía y Competitividad and co-financed by the European Regional Development Fund. The authors also acknowledge the financial support provided by Chilean Economic Development Agency, CORFO, with the contract no. 17PTECES-75830 under the framework of the project AtaMoS TeC, the Innova Chile - CORFO, project code: 17BPE3-83761, as well as CONICYT/ FONDAP/15110019 "Solar Energy Research Center" SERC-Chile.

References

Alonso-Montesinos, J., Batlles, F. J., Bosch, J. L., 2015. J. Beam, diffuse and global solar irradiance estimation with satellite imagery, Energy Conversion and Management 105, 1205-1212. https://doi.org/10.1016/j.enconman.2015.08.037

Alonso-Montesinos, J., Batlles, F. J., 2015. Solar radiation forecasting in the short- and medium-term under all sky conditions, Energy 83, 387-393. https://doi.org/10.1016/j.energy.2015.02.036

Boulifa, M., Adane, A., Rezagui, A., Ameur, E.Z., 2015. Estimate of the Global Solar Radiation by Cloudy Sky Using HRV Images. Energy Procedia 74, 1079-1089. https://doi.org/10.1016/j.egypro.2015.07.747

Dobos, A., Neises, T., Wagner, M., 2014. Advances in CSP simulation technology in the system advisor model. Energy Procedia 49, 2482–2489. http://dx.doi.org/10.1016/j.egypro.2014.03.263. https://doi.org/10.1016/j.egypro.2014.03.263

Escrig, H., Batlles, F. J., Alonso, J., Baena, F. M., Bosch, J. L., Salbidegoitia, I. B., Burgaleta, J. I., 2013. Cloud detection, classification and motion estimation using geostationary satellite imagery for cloud cover forecast. Energy 55, 853-859. https://doi.org/10.1016/j.energy.2013.01.054

Neises, T., Wagner, M. J., 2012. Simulation of Direct Steam Power Tower Concentrated Solar Plant. ASME 2012 6th International Conference on Energy Sustainability, Parts A and B, 499. https:// doi:10.1115/ES2012-91364

Rigollier C, Bauer O, Wald L., 2000. On the clear sky model of the ESRA e European Solar Radiation Atlas - with respect to the Heliosat method. Solar Energy 68, 33-48. https://doi.org/10.1016/S0038-092X(99)00055-9

Rigollier C, Lefvre, M., Wald L., 2004. The method Heliosat-2 for deriving shortwave solar radiation from satellite images. Solar Energy 77, 159-169. https://doi.org/10.1016/j.solener.2004.04.017

Wagner, M.J., 2008. Simulation and Predictive Performance Modeling of Utility-Scale Central Receiver System Power Plants. Thesis at the University of Wisconsin-Madison, Thesis at the University of Wisconsin-Madison.

Wagner, M.J., Gilman, P., 2011. Technical manual for the SAM physical trough model, Contract. NREL Report No. NREL/TP-5500-51825.